ELECTRIC TRANSITION STRENGTHS AND (e, e') FORM FACTORS FOR THE FIRST 2⁺ AND 3⁻ STATES IN THE EVEN Sn ISOTOPES

HOONG-CHIEN LEE

Atomic Energy of Canada Limited, Chalk River Nuclear Laboratories, Chalk River, Ontario, Canada, KOJ 1J0

Received 12 June 1975

Abstract: The Baranger formalism for the structure of spherical nuclei is applied to the first 2⁺ and 3⁻ states in the even Sn isotopes. Reduced electric transition strengths and (e, e') form factors for these states are calculated. The results compare satisfactorily with recently measured data.

1. Introduction

Recently, cross sections for (e, e') scattering with some even singly closed-shell nuclei in the $A \approx 50$, 90 and 120 mass regions as targets were measured ¹) with 209 MeV incident electrons; (e, e') form factors, with a range of momentum transfer from 0.5 fm^{-1} to 1.7 fm^{-1} , were deduced ¹) from these cross sections, for the first 2^+ and 3^- (and in some cases the 4^+) states in the nuclei studied. Moreover, these form factors were compared ¹) with theoretical predictions ^{1, 2}) in which the excited states are described as two-quasiparticle and particle-hole vibrations.

The results for the isotopes $^{116,\,120,\,124}$ Sn are of particular interest. At the first diffraction peaks of the quadrupole (e, e') form factors for the ground to 2_1^+ transitions the reported theoretical predictions are ≈ 50 times smaller than the measured values. This is in sharp contrast with the nuclei in the mass 50 and 90 regions, where the discrepancy is only a factor of 3 to 5, the theoretical predictions again being too small. On the other hand, the theoretically predicted magnitudes of the octopole form factors for the ground to 3_1^- transitions more or less agree with experiment at the first diffraction peaks. Furthermore, for both multipoles the predicted shapes of the form factors do not agree with those deduced experimentally.

In view of this rather serious failure of the theory, as applied to the Sn isotopes, it seems desirable that an independent calculation be performed. We report the result of such a calculation here. We find that for the Sn isotopes the predicted transition strength is only a factor of 2 to 3 smaller than the measured value. We also find that the theory is capable of reproducing the shapes of the experimentally deduced form factors. Furthermore, we show that using one value for the charge enhancement, $\Delta e = 0.2e$, all $B(E2; 0^+ \rightarrow 2_1^+)$ values and all except one $B(E3; 0^+ \rightarrow 3_1^-)$ value in the Sn isotopes, measured by Coulomb excitation, and to a lesser degree in accuracy, all inelastic electron scattering data, can be reproduced.

2. Results and discussion

As in ref. 2), the 2_1^+ and 3_1^- states are described in terms of particle vibrations, in the formalism of Baranger 3). For both neutrons and protons, twelve orbits from 2p, to lie are taken to be active. Spherical harmonic oscillator wave functions are used. The oscillator constant $\hbar\omega$ is taken to be proportional to $A^{-\frac{1}{3}}$, normalised to 8.3 MeV for ¹¹⁶Sn. Pairing effects are included in the calculations for the neutrons, but not for the protons, because the proton number for the Sn isotopes is magic. Thus the 2⁺ and 3⁻ states are composed of linear combinations of neutron twoquasiparticle and proton particle-hole components. Approximate values for most of the single-particle energies of these nuclei can be extracted from the spectra of neighbouring odd-mass nuclei 4). The single-particle energies used here are similar to those used by previous investigators 5, 6). The pairing and the multipole residual interactions are those of the K-matrix derived from the N-N interaction of Kahana, Lee and Scott ⁷). For each multipolarity (2⁺ or 3⁻) we allow the overall strength of the residual interaction to be varied to take into account renormalisation effects, such that for all isotopes studied the systematics of the excitation energies is best reproduced (see fig. 1). Briefly, the neutron pairing gap at the Fermi level is ≈ 1.5 MeV, and the smallest neutron two-quasiparticle energy is ≈ 3.1 MeV. Both of these decrease slightly as the mass number is increased. The smallest proton particle-hole energy is ≈ 5.0 MeV, which increases slightly with mass. It is a combination of these two effects that makes the transition strengths of the excited states decrease slightly with mass, as we will see below.

LOW ENERGY LEVELS OF EVEN Sn ISOTOPES

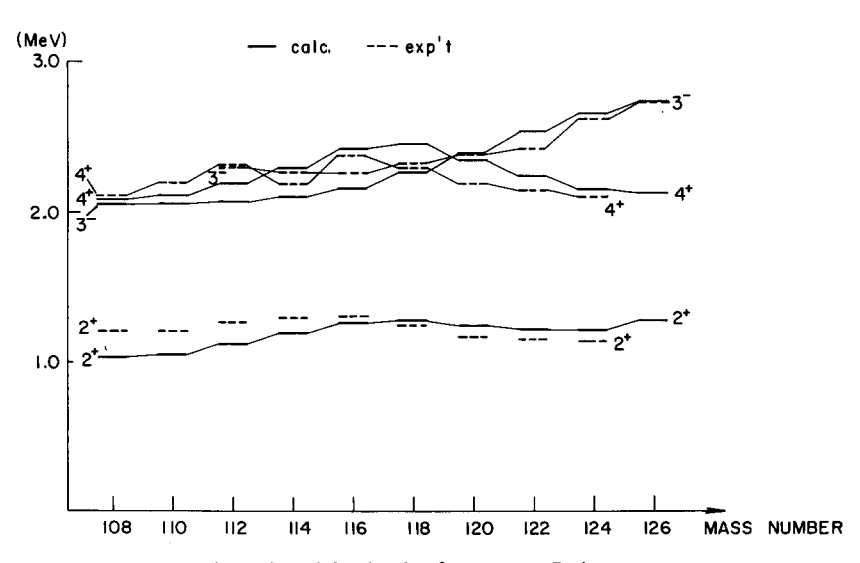


Fig. 1. Low-lying levels of even-mass Sn isotopes.

 $${\rm Table}\ l$$ Computed occupation amplitudes, or v-factors, for neutron orbits in $^{116}{\rm Sn}$ and $^{120}{\rm Sn}$

0.1%	Code no. for orbit	v-factor	
Orbit		¹¹⁶ Sn	¹²⁰ Sn
2p ₃	8	0.9944	0.9950
$1\hat{f}_{\frac{1}{4}}^{2}$	9	0.9937	0.9944
$2p_{\frac{1}{2}}^{2}$	10	0.9920	0.9930
lg,	11	0.9885	0.9903
2d ₄	12	0.9417	0.9547
lg ₃	13	0.8969	0.9227
3s ₄	14	0.8648	0.9016
2d ² 3	15	0.5458	0.6075
lh _¥	16	0.5255	0.5939
1h.*	17	0.2070	0.2254
$2f_{2}^{*}$	18	0.1128	0.1175
2f.² lių	19	0.0818	0.0825

Table 2 RPA amplitudes for neutron two-quasiparticle and proton particle-hole pairs of 2_1^+ states in $^{116}{\rm Sn}$ and $^{120}{\rm Sn}$

		¹¹⁶ Sn		¹²⁰ Sn	
		X	Y	X	Y
neut	ron 2qp				
18	8 a)	0.051 ^b)	0.029	0.047	0.027
17	9 ´	0.129	0.083	0.126	0.081
11	11	0.057	0.001	0.052	0.000
12	11	-0.129	-0.024	-0.108	-0.018
13	11	-0.051	-0.018	-0.042	-0.016
12	12	0.146	0.026	0.117	0.019
13	12	0.088	0.019	0.070	0.014
14	12	-0.266	-0.053	-0.212	-0.042
15	12	-0.156	-0.051	-0.142	-0.046
13	13	0.275	0.074	0.218	0.057
15	13	-0.427	-0.116	-0.384	-0.104
15	14	0.296	0.064	0.277	0.062
15	15	0.216	0.037	0.240	0.042
16	16	0.581	0.124	0.674	0.134
17	16	-0.068	-0.026	-0.080	-0.034
18	16	-0.158	-0.028	-0.167	-0.034
17	17	0.094	0.014	0.106	0.017
prote	on p-h				
18	8 a)	0.068	0.052	0.064	0.058
17	9 ′	0.152	0.119	0.149	0.118
12	11	-0.382	-0.218	-0.352	-0.203
13	11	-0.129	0.088	-0.123	-0.084

a) Each orbit is represented by its respective code number given in table 1.

b) Amplitudes with |X+Y| < 0.05 are not given.

TABLE 3 RPA amplitudes for neutron two-quasiparticle and proton particle-hole pairs of 3_1^- states in 116 Sn and 120 Sn

		¹¹⁶ Sn		¹²⁰ Sn	
		X	Y	X	Y
neuti	ron 2qp				
15	8	0.095	0.040	0.089	0.035
13	9	-0.084	-0.025	-0.074	-0.019
15	9	0.053	0.019	0.051	0.016
12	10	-0.061	-0.012	-0.056	-0.009
13	10	0.090	0.021	0.081	0.016
16	11	-0.230	-0.091	-0.215	-0.079
17	11	0.081	0.036	0.078	0.034
18	11	0.056	0.028	0.055	0.027
16	12	0.638	0.119	0.631	0.103
17	12	-0.089	-0.020	-0.089	-0.019
18	12	-0.106	-0.043	-0.105	-0.041
16	13	-0.325	-0.059	-0.318	-0.052
17	13	-0.278	-0.084	-0.281	-0.079
18	14	0.119	0.043	0.124	0.043
17	15	0.217	0.026	0.266	0.026
18	15	-0.060	-0.015	-0.069	-0.016
prote	on p-h				
12	8	-0.114	-0.057	-0.109	-0.053
13	8	-0.095	-0.049	-0.092	-0.045
15	8	0.125	0.070	0.118	0.065
12	9	0.096	0.039	0.090	0.036
13	9	-0.259	-0.107	-0.249	-0.099
14	9	-0.073	-0.038	-0.068	-0.035
15	9	0.093	0.047	0.086	0.043
12	10	-0.211	-0.081	-0.207	-0.075
13	10	0.264	0.101	0.266	0.094
16	11	-0.283	-0.125	-0.273	-0.116
17	11	0.053	0.038	0.048	0.034
18	11	0.050	0.036	0.047	0.033

The calculated occupation amplitudes, or v-factors, for the neutron orbits in 116 Sn and 120 Sn are shown in table 1. Amplitudes in the random phase approximation 3,8) (RPA) for the 2^+ states and 3^- states, in the same isotopes, are shown respectively in tables 2 and 3. Results for other isotopes are similar but have a systematic mass-dependence characteristic of the rising of the mean Fermi level through the neutron orbits, as the mass number increases. Results in the Tamm-Dancoff approximation 8) (TDA) are similar to those in RPA. But as usual they have weakened transition strengths, and as will be shown below, they have inferior mass dependence, compared to RPA results. The transition strength and (e, e') cross

90 H.-C. LEE

section depend on the transition charge density, which in our case is given by 9)

$$\rho_{\lambda}^{0 \to \lambda}(r) = \sum_{a \ge b} \frac{\hat{j}_a}{\lambda} (1 + \delta_{ab})^{-\frac{1}{2}} (u_a v_b + v_a u_b) (X_{ab}^{\lambda} + Y_{ab}^{\lambda}) g_{\text{eff}}(a || i Y_{\lambda}(r) || b), \tag{1}$$

$$(a||iY_{\lambda}||b) = -(-)^{j_b + \frac{1}{2} + \lambda} i^{l_b + \lambda - l_a} \frac{\hat{\lambda} \hat{j}_b}{\sqrt{4\pi}} \begin{pmatrix} j_a & j_b & \lambda \\ \frac{1}{2} & -\frac{1}{2} & 0 \end{pmatrix} R_a(r) R_b(r) \quad \text{if } l_a + l_b + \lambda \text{ even,}$$

$$= 0$$
 if otherwise, (2)

where a and b are labels of orbits; $u = \sqrt{1-v^2}$; $j_a = \sqrt{2j_a+1}$; $g_{\rm eff} = \Delta e/e$ for neutron orbits, and $g_{\rm eff} = 1 + \Delta e/e$ for proton orbits, Δe being the effective charge enhancement; and R(r) is the harmonic oscillator radial wave function. The transition strength is given by

$$B(E\lambda; 0 \to \lambda) = e^{2}(2\lambda + 1) \left(\int r^{\lambda + 2} \rho_{\lambda}^{0 \to \lambda}(r) dr \right)^{2}.$$
 (3)

The (e, e') Coulomb form factor, when distortion on the electron waves is ignored, is given by

$$|F_{\lambda}(q^2)|^2 = \frac{4\pi}{Z^2} (2\lambda + 1) \left(\int \rho^{0 \to \lambda}(r) j_{\lambda}(qr) r^2 dr \right)^2. \tag{4}$$

The density, the transition strength and the form factor are calculated using the computer code MICRODENS 9).

Cross sections for (e, e') were also calculated in the distorted-wave Born approximation, where a modified version of the code DUELS, written by the Yale-Duke-Ohio group ^{10, 11}), were used. In this case the "form factor" squared is the cross section normalized to the Mott cross section

$$|F(q^2)|^2 = \frac{d\sigma}{d\Omega} \left/ \left(\frac{d\sigma}{d\Omega} \right)_{Mott} = \frac{d\sigma}{d\Omega} \left/ \left[\frac{(Z\alpha)^2 \sin^2 \frac{1}{2}\theta}{4p_i^2 \cos^4 \frac{1}{2}\theta} \right],$$
 (5)

where $\alpha \approx \frac{1}{137}$ is the fine structure constant, θ is the scattering angle, and p_i is the initial electron momentum. The momentum transfer is given by

$$q^2 = |\mathbf{p}_i - \mathbf{p}_f|^2 = p_i^2 + p_f^2 - 2p_i p_f \cos \theta,$$

where p_f is the final electron momentum.

The calculated 0_1^+ to 2_1^+ and to 3_1^- transition strengths expressed in the appropriate Weisskopf units $[1 \text{ W.u.}(\lambda) = [(2\lambda+1)/4\pi][3/(3+\lambda)]^2(1.2A^{\frac{1}{2}})^{2\lambda}e^2 \cdot \text{fm}^{2\lambda}]$ are shown in fig. 2 and compared with data extracted from Coulomb excitation experiments $^{12, 13}$). The solid (dashed) lines represent the RPA (TDA) results, where a charge enhancement of $\Delta e = 0.2e$ ($\Delta e = 0.45e$) has been assigned to the active protons

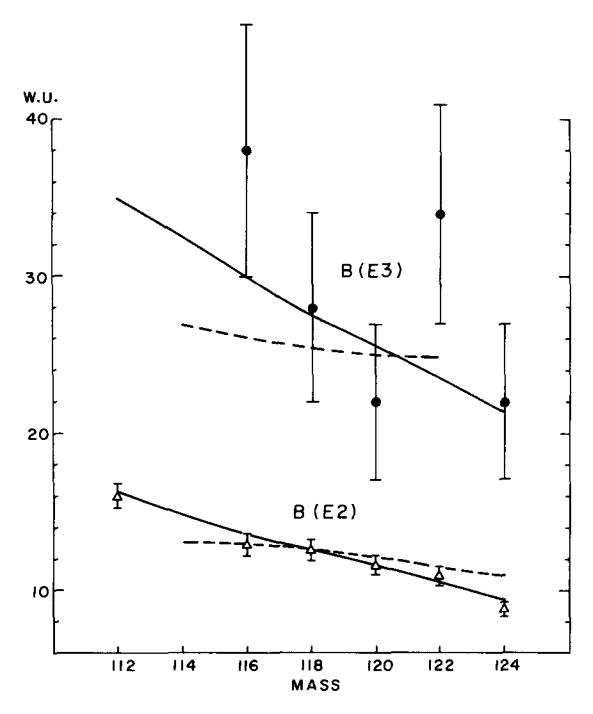


Fig. 2. Calculated values of $B(E2; 0_1^+ \to 2_1^+)$ and $B(E3; 0_1^+ \to 3_1^-)$ in RPA, $\Delta e = 0.20e$ (solid lines) and in TDA, $\Delta e = 0.45e$ (dotted lines). Experimental values for B(E2) are from ref. ¹²), and those for B(E3) are from ref. ¹³).

and neutrons. The RPA results are better as the mass dependence of the data 12) is well reproduced. We shall discuss only the RPA results in the following. For the B(E2) values the theoretical results shown in fig. 2 are about 3.1 times larger than those obtained when no charge enhancement is assigned. This is similar to the results reported in ref. 1) for nuclei in the mass 50 and 90 regions, but very different from those for the Sn isotopes, where without charge enhancement the theoretical B(E2) values were reported to be more than twenty times smaller than the corresponding measured values. Actually it would be more than a little surprising if such a large discrepancy between theory and experiment indeed existed, since the measured E2 strengths for the Sn isotopes are not particularly strong, being only about 10-15 W.u. The computed B(E3) values shown in fig. 2 are about 2.3 times larger than those obtained with no charge enhancement.

The calculated (e, e') form factors for the 0_1^+ to 2_1^+ transitions in 116 Sn and 120 Sn are plotted in fig. 3 and compared with available data. The same ($\Delta e = 0.2e$) charge enhancement is used. Without enhancement the predictions are a factor of ≈ 3.1 smaller but the shape of the form factors, as a function of the momentum transfer q does not change. In fig. 3 (as well as in fig. 4) the solid curves are calculated using distorted waves for the electrons. The dash curves show results obtained in the Born

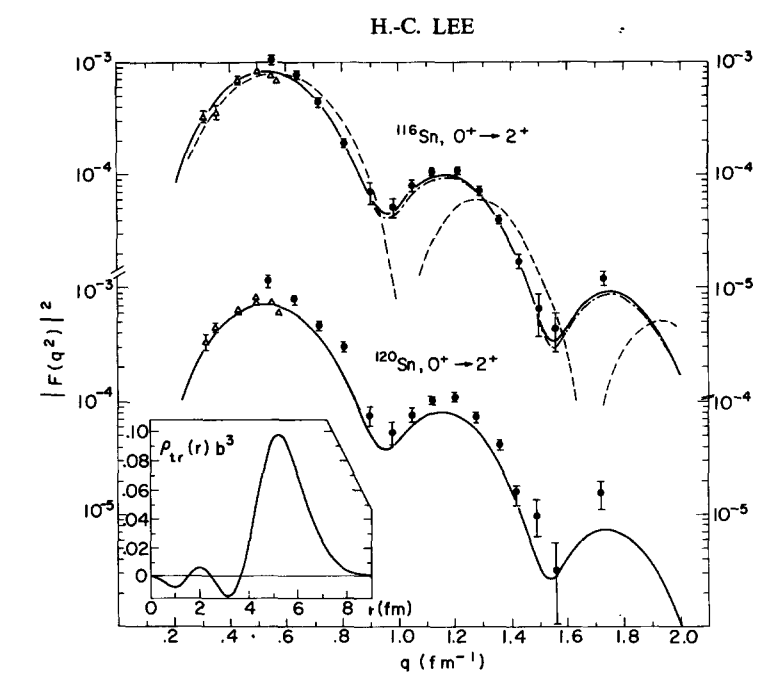


Fig. 3. The (e, e') form factors for the $0_1^+ \to 2_1^+$ transitions in 116,120 Sn. The curves are calculated using distorted waves for the electrons (solid line), and using plane waves for the electrons (dotted line). The dot-dash curve is obtained using a ground-state density obtained in a density-dependent Hartree-Fock calculation 15). The open triangles are experimental points from ref. 16) and the solid circles are data from ref. 1). The inset shows the calculated $0_1^+ \to 2_1^+$ transition density in 116 Sn; b = 2.235 fm.

approximation. As expected the latter is not reliable at and beyond the first diffraction minimum. In the distorted wave calculation the ground-state charge density is represented by a two-parameter Fermi distribution ¹⁴). A more sophisticated ground-state charge density, obtained in a density-dependent Hartree-Fock calculation 15), and giving a better account of the elastic electron scattering data, is used. This density produces little change (fig. 3, dash-dot-dash curve) in the (e, e') result, however. The triangles in fig. 3 (and fig. 4) are those of Curtis et al. 16) obtained with 60 MeV incident electrons. The solid circles are those of Phan-Xuan-Ho et al. 1) with 209 MeV electrons. For 116Sn the theoretical result reproduces the data points very well. For ¹²⁰Sn the theoretical curve does not fit all the data points as well. For the latter nucleus it is in fact not possible to fit both sets of data simultaneously since there is a significant difference between the two at $q \approx 0.55$ fm⁻¹. The data of Curtis et al. show a slight decrease in the transition strength going from ¹¹⁶Sn to ¹²⁰Sn, in agreement with the direct B(E2) measurements ¹²) at zero momentum transfer (see fig. 2). In contrast the data of Phan-Xuan-Ho et al. show a slight increase in strength.

The form factors for the 0_1^+ to 3_1^- transitions in $^{116,\ 120}$ Sn are shown in fig. 4. The theoretical curves are obtained again by setting $\Delta e=0.2e$. The results reproduce

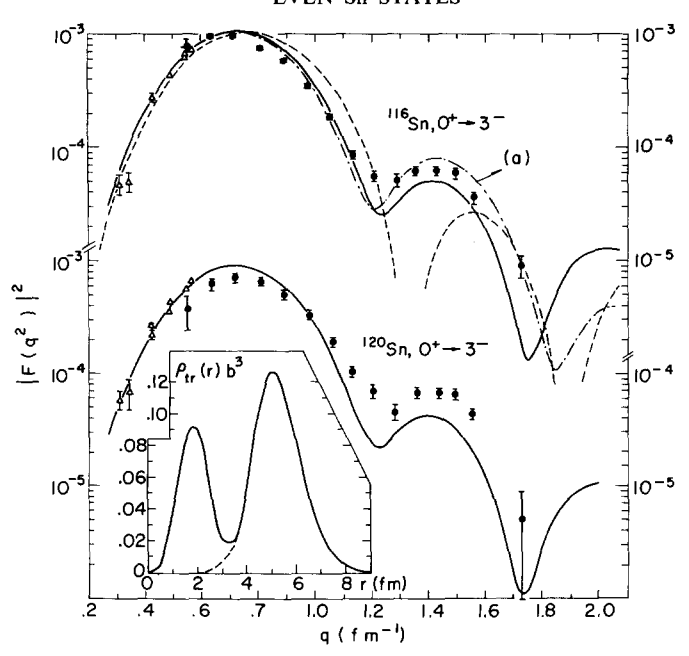


Fig. 4. The (e, e') form factors for the $0_1^+ \rightarrow 3_1^-$ transitions in ^{116, 120}Sn. (For notation see fig. 3.) Here curve (a) is obtained using a transition density the same as the one shown in the inset but with the smaller peak cut off at the dashed line.

the data fairly well. The serious disparity between the theoretically predicted shape and the observed shape reported in ref. ¹) is not evident here. We point out that for ¹²⁰Sn again there is a significant difference between the two sets of data at $q \approx 0.55$ fm⁻¹, suggesting a difference in the normalisation procedures [†] used in the two experiments.

The calculated transition densities for the quadrupole and octupole transitions in 116 Sn are shown in the insets of figs. 3 and 4, respectively. These have more structure than that usually adopted for phenomenological analyses, which is proportional to the derivative of a Fermi density distribution 17). The octopole density in fig. 4 is particularly interesting as it exhibits a prominent peak in the interior in addition to the usual one centering near the nuclear surface. In order to examine the effect of this second peak we repeated the calculation for 116 Sn excluding the contribution from the interior. This procedure reduces the B(E3) value by less than 1%. The new form factor is shown as curve (a) in fig. 4. We see that beyond the first diffraction minimum, this latter result is clearly distinct from that obtained with the full density. However, in so far as fitting the presently available data is concerned neither result is distinctly superior to the other.

[†] For normalization purposes a three-parameter Gaussian model is used for the ground-state charge density to calculate the elastic form factor in ref. ¹). In ref. ¹⁶) a two-parameter Fermi density is used.

References

- 1) Phan-Xuan-Ho, J. Bellicard, Ph. Leconte and I. Sick, Nucl. Phys. A210 (1973) 189
- 2) V. Gillet, B. Giraud and M. Rho, Phys. Rev. 178 (1969) 178; and CEN Saclay, report DPh-T/72-22
- 3) M. Baranger, Phys. Rev. 120 (1960) 957
- B. L. Cohen, Nuclear structure, Dubna Symp., 1968 (IAEA, Vienna, 1968);
 P. E. Cavanagh, C. F. Coleman, A. G. Hardacre, G. A. Gard and T. F. Turner, Nucl. Phys. A141 (1970) 97
- D. M. Clement and E. U. Baranger, Nucl. Phys. A120 (1968) 25;
 E. U. Baranger, Advances in physics, vol. 4, ed. M. Baranger and E. Vogt (Plenum Press, New York, 1971)
- 6) H. C. Lee and K. Hara, Phys. Rev. C3 (1971) 325
- 7) S. Kahana, H. C. Lee and C. K. Scott, Phys. Rev. 180 (1969) 956
- 8) G. E. Brown, Unified theory of nuclear models and forces (North-Holland, Amsterdam, 1967)
- H. C. Lee, Nuclear charge, convection current and magnetization current densities (Atomic Energy of Canada Limited report no. 4839, 1975)
- 10) J. F. Ziegler, report Yale-2726 E-49 (USAEC, TID-4500, 1967)
- 11) S. T. Tuan, L. E. Wright and D. S. Onley, Nucl. Instr. 60 (1968) 70
- 12) P. H. Stelson, F. K. McGowan, R. L. Robinson and W. T. Milner, Phys. Rev. C2 (1970) 2015
- 13) D. G. Alhazov, Y. P. Gangrskii, I. K. Lemberg and Y. J. Undralov, Izv. Akad. Nauk SSSR (ser. fiz.) 28 (1964) 232
- 14) H. R. Collard, L. R. B. Elton and R. Hofstadter, Landold-Börnstein numerical and functional relationship in science and technology, New series, group 1, vol. 2 (Springer Verlag, Berlin, 1967)
- 15) X. Campi, D. W. L. Sprung and J. Martorell, Nucl. Phys. A223 (1974) 541
- 16) T. H. Curtis, R. A. Eisenstein, D. W. Madsen and C. K. Bockelman, Phys. Rev. 184 (1969) 1162
- 17) L. J. Tassie, Nuovo Cim. 5 (1957) 1497